NOTE: U_I in the following notes is used instead of U to represent the normalized electrostatic potential in the semiconductor.

I_D–V_D "Exact" formulation

The relationship between the exact formulation and the foregoing theories is much the same as the relationship between charge analysis and the δ-depletion approach used in establishing the MOS-C C-V_G' characteristics. $Q_N(y)$ is no longer thought of as a δ-function but is deduced from electrostatic computations which treat the x-direction band bending in the channel. Furthermore, the exact formulation retains both the drift and diffusion components in the computation of I_D. As a consequence of the increased theoretical sophistication one can eliminate a major failing present in the simpler theories. Conceptually, leads ohmically connected to a semiconductor can be thought of as tying directly into the semiconductor Fermi level. When the source is grounded and the drain $V_D > 0$ biased, the Fermi level of the drain island is lowered by an energy qV_D relative to the Fermi level of the source island. This does NOT automatically imply that the electrostatic potential increases by an amount V_D at y=L relative to y=0. In other words, externally applied voltages set the <u>electrochemical</u> potential difference between points in a semiconductor, not the electrostatic potential difference. By invoking the Q_N δ-function approximation and ignoring the diffusion current one essentially equates the electrochemical and electrostatic potential variation in the y-direction. This simplification is no longer necessary in the exact formulation.

As implied in the preceding paragraph, the exact formulation involves Fermi level and quasi-Fermi level considerations. Addressing ourselves to the positional variation of these levels we note that setting $J = J_{Ny}$ in the MOST channel (general simplification (6), section 11.2.1) is equivalent to assuming $J_P = 0$ and $J_{Nx} = 0$ in a n-channel device. However,

$$J_P = \mu_p P \nabla F_P = 0 \implies F_P = \text{constant} = E_F$$

$$J_{Nx} = \mu_n N \, dF_N/dx = 0 \implies F_N = F_N(y) = \text{constant in the x-direction}$$

In other words, based on the $J = J_{Ny}$ simplification, the majority carrier (hole) quasi-Fermi level forms an energy surface which is constant everywhere under the MOST gate. The bulk minority carrier (electron) quasi-Fermi level forms an energy surface in the channel which is constant in the x-direction but slopes in the y-direction from the source to the drain. At the source F_N must line-up with the source Fermi level; at the drain F_N must line-up with the drain Fermi level (see Fig. 11.8). In the semiconductor bulk F_N must of course come back up to the bulk Fermi level, E_F; i.e., F_N will exhibit an x-dependence at some point exterior to the channel and a small J_{Nx} current will flow from the semiconductor surface into the semiconductor bulk. Because of the low carrier concentrations involved, however, little error is introduced if one assumes $F_N = F_N(y) = \text{constant}$ independent of x everywhere. Taking $F_N = F_N(y)$ everywhere under the MOST gate we can write

$$U_N(y) = \left[E_i^{(B)} - F_N(y)\right]/kT = \left[E_i^{(B)} - E_F\right]/kT + \left[E_F - F_N(y)\right]/kT$$
$$= U_F + \xi(y) \qquad (11.32)$$

$$\xi(y) \equiv \left[E_F - F_N(y)\right]/kT \qquad (11.33)$$

The newly introduced $\xi(y)$ parameter can be thought of as the normalized electrochemical potential at any given point in the channel. At the source $\xi(y)=0$; at the drain $\xi(y)=V_D/(kT/q) \equiv U_D$.

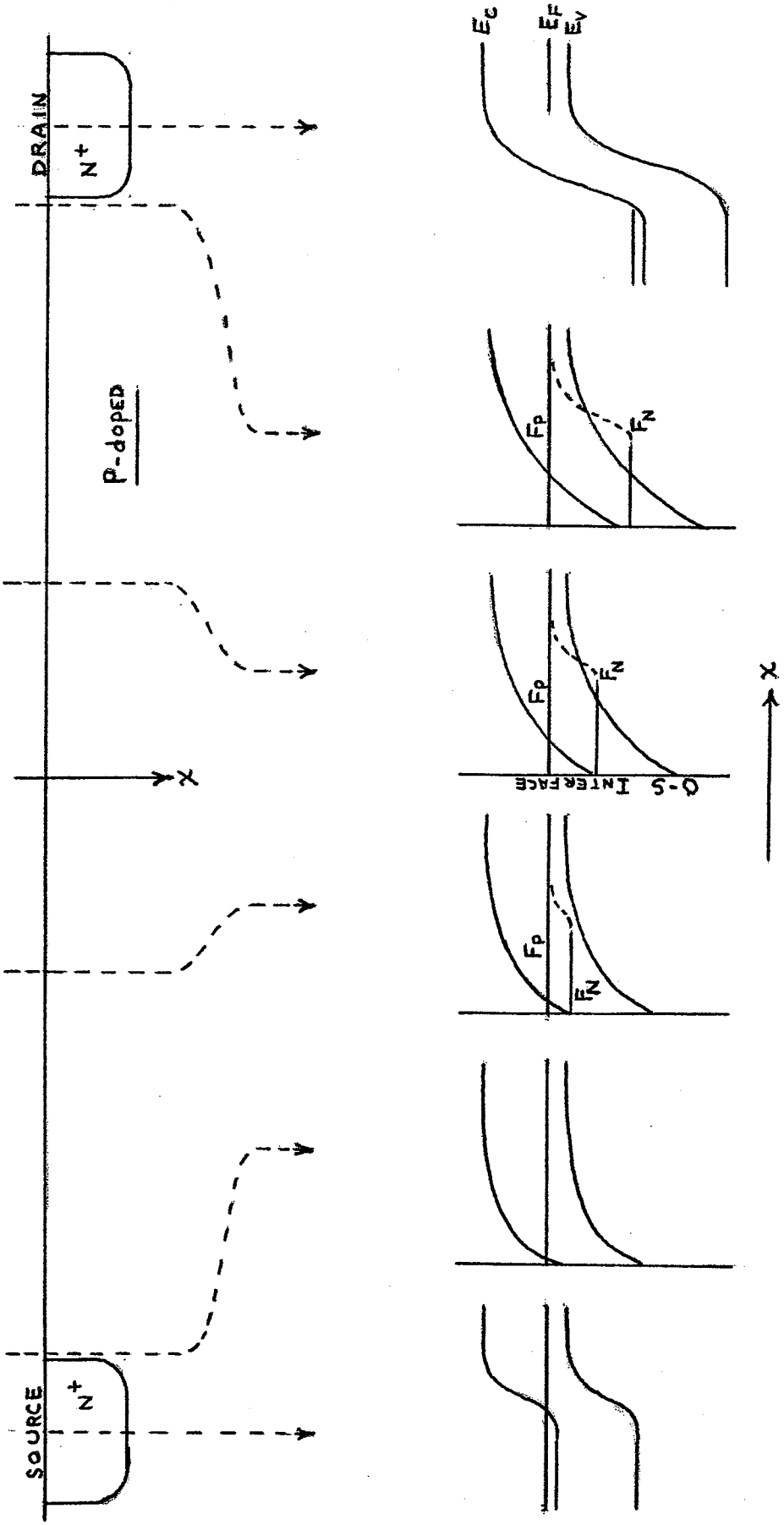

Fig. 11.8 Band bending and position of the carrier quasi-Fermi levels along selected y=constant planes in the MOST structure.

The remainder of the exact formulation involves straightforward algebra. Since

$$N(x,y) = n_i e^{U_I - U_N} = n_i e^{U_I(x,y) - U_F - \xi(y)} \qquad \text{(n-channel device)} \tag{11.34a}$$

$$P(x,y) = n_i e^{U_P - U_I} = n_i e^{U_F - U_I(x,y)} \tag{11.34b}$$

and, under the gradual channel approximation,

$$\nabla \cdot \vec{\mathcal{E}} \simeq \frac{\partial \mathcal{E}_x}{\partial x} = -\frac{\partial^2 U_I}{\partial x^2} \tag{11.35}$$

we can write

$$\frac{\partial^2 U_I}{\partial x^2} = \frac{1}{2L_D^2}\left(e^{U_I - U_F - \xi(y)} - e^{U_F - U_I} + e^{U_F} - e^{-U_F}\right) \tag{11.36}$$

The constancy of ξ in the x-direction permits eq.(11.36) to be integrated in a routine manner.

$$\frac{\partial U_I}{\partial x} = -\hat{U}_{IS}\frac{F(U_I, U_F, \xi)}{L_D} \tag{11.37}$$

$$F(U_I, U_F, \xi) = \left[e^{U_F}(e^{-U_I} + U_I - 1) + e^{-U_F}(e^{U_I - \xi} - U_I - e^{-\xi})\right]^{1/2} \tag{11.38}$$

We can now determine $Q_N(y)$.

$$Q_N(y) = -q\int_0^{x_f} N(x,y)dx \simeq -qn_i \int_0^{\infty}(e^{U_I - U_F - \xi} - e^{-U_F - \xi})dx \tag{11.39a}$$

$$= -qn_i L_D \int_0^{U_{IS}} \frac{(e^{U_I - U_F - \xi} - e^{-U_F - \xi})dU_I}{F(U_I, U_F, \xi)} \tag{11.39b}$$

The introduction of the $n_i \exp(-U_F - \xi)$ term in the above equations is merely a maneuver to permit integration into the semiconductor

bulk. Without this term Q_N formally blows up as $U_I \rightarrow 0$. In an actual computation, however, one terminates U_I at some value > 0, usually $U_I = U_F$, thereby completely negating the importance of this term. $\hat{U}_{IS}$ was dropped in transforming from x to U_I in eq.(11.39b) with the understanding that only $U_{IS} > 0$ values are of interest in n-channel operation.

Turning to the current derivation proper we have

$$J = J_{Ny} = \mu_n N \, dF_N/dy = -kT\mu_n N \, d\xi/dy \tag{11.40}$$

$$I_D = -Z \int_0^{x_c} J_{Ny} dx = Z\bar{\mu}_n kT \frac{d\xi}{dy} \int_0^{x_c} N(x,y)dx \tag{11.41a}$$

$$= -Z\bar{\mu}_n \frac{kT}{q} Q_N \frac{d\xi}{dy} \tag{11.41b}$$

Separating variables, integrating over the length of the channel, noting $kTn_iL_D = (C_o/2)(K_S x_o/K_O L_D)(kT/q)^2$, and remembering I_D is a constant independent of y, one obtains

$$\left[\left[I_D = \frac{Z\bar{\mu}_n C_o}{2L}\left(\frac{K_S x_o}{K_O L_D}\right)\left(\frac{kT}{q}\right)^2 \int_0^{U_D} d\xi \int_0^{U_{IS}} \frac{e^{U_I - U_F - \xi} - e^{-U_F - \xi}}{F(U_I, U_F, \xi)} dU_I \right]\right] \tag{11.42}$$

$$\ldots V_G' > 0$$

$$U_D \equiv V_D/(kT/q) > 0$$

where the functional relationship between U_{IS} and ξ is determined by

$$V_G' = \frac{kT}{q}\left[U_{IS} + \hat{U}_{IS} \frac{K_S x_o}{K_O L_D} F(U_{IS}, U_F, \xi)\right] \tag{11.43}$$

Taken together eqs.(11.42) and (11.43) constitute a complete solution for $I_D(V_G', V_D)$. To compute I_D for a given V_G'--V_D data set one must first solve eq.(11.43) by an iteration process to obtain U_{IS} vs. ξ at various points along the channel. This

information is then substituted into eq.(11.42) and the double integration performed using numerical methods.

The most intriguing aspect of the exact formulation is the automatic saturation of the predicted I_D-V_D characteristics at large V_D values. This negates the need to define a V_{DS} and the theory can be utilized for all drain voltages $>$ 0 (n-channel devices) even though one of the major theoretical assumptions, namely $\mathcal{E}_y \ll \mathcal{E}_x$, is explicitly violated in the structure above pinch-off. This automatic saturation results of course from the inclusion of the diffusion current and the proper handling of the applied voltage boundary conditions. The reader will also note the absence of a turn-on voltage in the exact formulation. A sharply defined turn-on point is in reality a convenient fiction necessitated by the δ-depletion approximation utilized in the simpler theories. As correctly predicted by the exact theory, a surface current can be observed at surface potentials slightly below $U_{IS} = 2U_F$ and "turn-on" is not an abrupt phenomenon; the current actually increases to a significant magnitude over a small range in gate potentials.

Solid-State Electronics Vol. 26. No. 2, pp. 143–147, 1983
Printed in Great Britain.

0038-1101/83/020143-05$03.00/0
Pergamon Press Ltd.

SIMPLIFIED LONG-CHANNEL MOSFET THEORY

R. F. PIERRET and J. A. SHIELDS
School of Electrical Engineering, Purdue University, W. Lafayette, IN 47907, U.S.A.

(*Received* 10 *April* 1982; *in revised form* 19 *June* 1982)

Abstract—The now-classic and highly accurate double-integral expression for the drain current flowing in long-channel MOSFET's is shown to be reducible to a completely equivalent single-integral expression. The single-integral expression is used in turn to straightforwardly establish the approximate closed-form results commonly known as the bulk-charge and charge-sheet relationships. Sample computations which illustrate the general utility of the single-integral expression are also presented.

1. INTRODUCTION

The double-integral relationship established by H. C. Pao and C. T. Sah[1] is generally accepted as a precise representation of the static characteristics derived from long-channel MOSFET's. The relationship is routinely cited in authoritative textbooks[2] and review articles[3]. The Pao–Sah result, moreover, has been used as a starting point in deriving approximate closed-form relationships and in evaluating the accuracy of such relationships[4, 5]. One advantage of the Pao–Sah formulation is that it is continuously valid in all biasing regions including weak inversion and saturation. A major drawback is the complexity and time consuming nature of the numerical calculations required in evaluating a double-integral relationship.

The primary purpose of this paper is to point out that the Pao–Sah double-integral expression can be transformed into a completely equivalent single-integral expression. The single-integral result automatically leads to drastically reduced computational times. Details of the mathematical simplification are presented in the next section along with the development of closed-form approximations, the "charge-sheet" and "bulk-charge" expressions[5, 6], which follow in a very direct manner from the single-integral result. Sample computations involving both the single-integral and charge-sheet expressions are presented in Section 3; the final section contains a summary of results and concluding comments.

2. THEORY

Single-integral derivation

The Pao–Sah result for the drain current (I_D) flowing in an n-channel MOSFET can be written in the following form†:

$$I_D = \frac{Z\bar{\mu}_n C_0}{L}\frac{x_0'}{2L_D}\left(\frac{kT}{q}\right)^2\int_0^{U_D}\int_0^{U_S}\frac{e^{U-U_F-\xi}-e^{-U_F-\xi}}{F(U, U_F, \xi)}\,dU\,d\xi \tag{1}$$

where

$$V_G' = \frac{kT}{q}\left[U_S + \frac{x_0'}{L_D}F(U_S, U_F, \xi)\right] \geq 0 \tag{2}$$

$$V_D = \frac{kT}{q}U_D \geq 0 \tag{3}$$

and

$$F(U, U_F, \xi) \equiv [e^{U_F}(e^{-U}+U-1) + e^{-U_F}(e^{U-\xi}-U-e^{-\xi})]^{1/2}. \tag{4}$$

Z is the channel width, L the channel length, $\bar{\mu}_n$ the electron effective mobility in the surface channel, L_D is the intrinsic Debye length, k Boltzmann's constant, T temperature, and q the magnitude of the electronic charge. $C_0 = K_0\epsilon_0/x_0$ is the oxide capacitance per unit area; K_0 is the oxide dielectric constant, ϵ_0 the permittivity of free space, and x_0 the oxide thickness. $x_0' \equiv K_S x_0/K_0$, where K_S is the semiconductor dielectric constant. V_D is of course the applied drain voltage and V_G' the ideal device gate voltage (the gate voltage less the flat band voltage). The source and back of the structure are assumed to be grounded.

Normalized potentials appearing in the formulation are defined as follows:

$$U = [E_i(\text{bulk}) - E_i(x)]/kT \tag{5}$$

$$U_S = U|_{x=0} \tag{6}$$

$$U_F = [E_i(\text{bulk}) - E_F]/kt = \ln(N_A/n_i) \tag{7}$$

and

$$\xi = [E_F - F_N(y)]/kT \tag{8}$$

x is taken to be the coordinate directed into the semiconductor, with $x = 0$ at the oxide-semiconductor interface; y is the coordinate parallel to the oxide-semiconductor interface, with $y = 0$ at the source contact. E_i is the intrinsic Fermi energy, E_F the bulk Fermi energy, $F_N(y)$ the electron quasi-Fermi level in the surface channel, N_A the bulk acceptor doping and n_i the intrinsic carrier concentration.

†The form presented here differs slightly from the Ref. [1] result in that the $U = 0$ value of the electron concentration is subtracted from the electron concentration at all points in the surface channel. This minor modification employed by J. R. Brews[5] and other authors permits one to extend the lower integration limit on U to $U = 0$.

The key to the simplification of the double-integral result is the observation that

$$\frac{\partial F}{\partial \xi} = -\frac{e^{U-U_F-\xi} - e^{-U_F-\xi}}{2F(U, U_F, \xi)}. \tag{9}$$

Equation (1) therefore becomes

$$I_D = -\frac{Z\bar{\mu}_n C_0}{L}\frac{x_0'}{L_D}\left(\frac{kT}{q}\right)^2 \int_0^{U_D}\int_0^{U_S}\frac{\partial F}{\partial \xi}\,dU\,d\xi. \tag{10}$$

The obvious next step is to interchange the order of the integrations. Some care must be exercised in effecting this interchange to obtain the correct integration limits. With reference to Fig. 1 one concludes

$$\int_0^{U_D}\left[\int_0^{U_S}\frac{\partial F}{\partial \xi}\,dU\right]d\xi = \int_0^{U_{S0}}\left[\int_0^{U_D}\frac{\partial F}{\partial \xi}\,d\xi\right]dU + \int_{U_{S0}}^{U_{SL}}\left[\int_{\xi_0}^{U_D}\frac{\partial F}{\partial \xi}\,d\xi\right]dU \tag{11}$$

where U_{S0} is U_S evaluated at the source ($x = 0$), U_{SL} is U_S evaluated at the drain ($x = L$), and $\xi_0(y)$ for a given $U_S(y)$ is specified by the gate voltage relationship (eqn 2). Changing variables from ξ to F of course yields a perfect differential and

$$\int_0^{U_D}\int_0^{U_S}\frac{\partial F}{\partial \xi}\,dU\,d\xi = \int_0^{U_{S0}}[F(U, U_F, U_D) - F(U, U_F, 0)]\,dU + \int_{U_{S0}}^{U_{SL}}[F(U, U_F, U_D) - F(U, U_F, \xi_0)]\,dU \tag{12a}$$

or

$$\int_0^{U_D}\int_0^{U_S}\frac{\partial F}{\partial \xi}\,dU\,d\xi = \int_0^{U_{SL}}F(U, U_F, U_D)\,dU - \int_0^{U_{S0}}F(U, U_F, 0)\,dU - \int_{U_{S0}}^{U_{SL}}F(U_S, U_F, \xi_0)\,dU_S. \tag{12b}$$

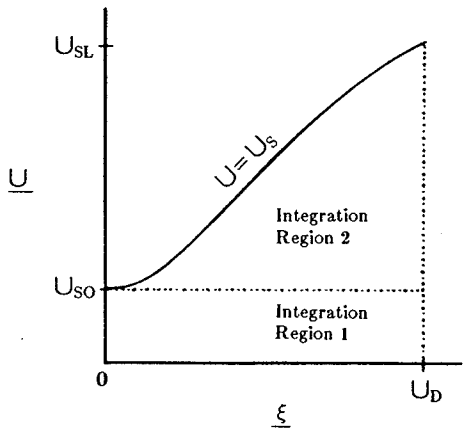

Fig. 1. The $U-\xi$ integration plane. Note the two regions of integration when the integration on ξ is performed first.

However, referring to eqn (2), we note

$$F(U_S, U_F, \xi_0) = \frac{V_G' - (kT/q)U_S}{(kT/q)(x_0'/L_D)} \tag{13}$$

and therefore

$$\int_{U_{S0}}^{U_{SL}}F(U_S, U_F, \xi_0)\,dU_S = \frac{q}{kT}\frac{L_D}{x_0'}\int_{U_{S0}}^{U_{SL}}\left(V_G' - \frac{kT}{q}U_S\right)dU_S \tag{14a}$$

$$= \frac{q}{kT}\frac{L_D}{x_0'}\left[V_G'(U_{SL} - U_{S0}) - \frac{1}{2}\frac{kT}{q}(U_{SL}^2 - U_{S0}^2)\right] \tag{14b}$$

Finally, combining eqns (10), (12b) and (14b), we obtain the desired result

$$I_D = \frac{Z\bar{\mu}_n C_0}{L}\left[V_G'(V_{SL} - V_{S0}) - \frac{1}{2}(V_{SL}^2 - V_{S0}^2)\right] + \frac{Z\bar{\mu}_n C_0}{L}\frac{x_0'}{L_D}\left(\frac{kT}{q}\right)^2\left[\int_0^{U_{S0}}F(U, U_F, 0)\,dU - \int_0^{U_{SL}}F(U, U_F, U_D)\,dU\right] \tag{15}$$

where the surface potentials at the source and drain are computed respectively from

$$V_G' = \frac{kT}{q}\left[U_{S0} + \frac{x_0'}{L_D}F(U_{S0}, U_F, 0)\right] \tag{16a}$$

$$V_G' = \frac{kT}{q}\left[U_{SL} + \frac{x_0'}{L_D}F(U_{SL}, U_F, U_D)\right] \tag{16b}$$

and

$$V_{S0} = \frac{kT}{q}U_{S0} \tag{17a}$$

$$V_{SL} = \frac{kT}{q}U_{SL} \tag{17b}$$

As previously defined, $V_D = (kT/q)U_D$.

Closed-form approximations

The eqn (15) result is highly suggestive of the simpler closed-form MOSFET theories used extensively in first-order analyses. Seeking a closed-form result, we note that, to a high degree of precision,

$$F(U, U_F, \xi) \cong [e^{U_F}(U-1) + e^{U-U_F-\xi}]^{1/2} \tag{18}$$

for the range of parameters encountered in n-channel MOSFET operation. Unfortunately, the eqn (18) form of the F-function when substituted into eqn (15) still does not yield a closed-form result. A further simplification of the F-function is clearly required.

One approach, which leads to the bulk-charge result, is to totally neglect the $\exp(U - U_F - \xi)$ term in eqn (18).

Specifically, substituting $F(U, U_F, \xi) = \sqrt{(U)} \exp(U_F/2)$ into eqn (15) and integrating yields

$$I_D = \frac{Z\bar{\mu}_n C_0}{L}\left[V'_G(V_{SL} - V_{S0}) - \frac{1}{2}(V_{SL}^2 - V_{S0}^2) - \frac{2}{3}\frac{x'_0}{L_D}\sqrt{\left(\frac{kT}{q}\right)\left(\frac{N_A}{n_i}\right)}(V_{SL}^{3/2} - V_{S0}^{3/2})\right]. \quad (19)$$

Equation (19) reduces to the standard bulk-charge expression if, following the usual formulation, one further approximates the potentials at the source and drain ends of the channel to be $V_{S0} = (kT/q)(2U_F)$ and $V_{SL} = (kT/q)(2U_F) + V_D$, respectively.

A second, more carefully structured, F-function approximation leads in a straightforward manner to the closed-form charge-sheet expression. The charge-sheet result is of special interest herein because it is reported to be highly accurate and continuously valid in all biasing regions including weak inversion and saturation. To obtain the charge-sheet result we introduce the approximation,

$$F(U, U_F, \xi) \cong e^{U_F/2}[\sqrt{(U-1)} + \alpha(U_S, U_F, \xi)e^{U-2U_F-\xi}] \quad (20)$$

where $\alpha(U_S, U_F, \xi)$ is chosen such that $F(U, U_F, \xi)$ computed from eqn (20) precisely matches $F(U, U_F, \xi)$ computed from eqn (18) [or eqn 4] at $U = U_S$. In other words, the proposed approximation is exact when $F(U, U_F, \xi)$ is at its maximum.†

Obviously, the precise functional form of $\alpha(U_S, U_F, \xi)$ could be determined by first evaluating the two F-functions [eqns 18 and 20] at $U = U_S$ and then equating the two expressions. As it turns out, however, the precise functional form of α is not required in the derivation.

Substituting the eqn (20) approximation into the eqn (15) integrals, one obtains

$$\int_0^{U_{S0}} F(U, U_F, 0)\,dU - \int_0^{U_{SL}} F(U, U_F, U_D)\,dU = e^{U_F/2}\left[\alpha_0\int_0^{U_{S0}} e^{U-2U_F}\,dU - \alpha_L\int_0^{U_{SL}} e^{U-2U_F-U_D}\,dU - \int_{U_{S0}}^{U_{SL}}\sqrt{(U-1)}\,dU\right] \quad (21a)$$

$$\cong e^{U_F/2}\left[\alpha_0 e^{U_{S0}-2U_F} - \alpha_L e^{U_{SL}-2U_F-U_D} - \frac{2}{3}(U_{SL}-1)^{3/2} + \frac{2}{3}(U_{S0}-1)^{3/2}\right] \quad (21b)$$

where $\alpha_0 \equiv \alpha(U_{S0}, U_F, 0)$ and $\alpha_L \equiv \alpha(U_{SL}, U_F, U_D)$. Next we note that eqns (16a) and (16b) can be written in the alternative form

$$V'_G = \frac{kT}{q}\left\{U_{S0} + \frac{x'_0}{L_D}e^{U_F/2}[\sqrt{(U_{S0}-1)} + \alpha_0 e^{U_{S0}-2U_F}]\right\} \quad (22a)$$

and

$$V'_G = \frac{kT}{q}\left\{U_{SL} + \frac{x'_0}{L_D}e^{U_F/2}[\sqrt{(U_{SL}-1)} + \alpha_L e^{U_{SL}-2U_F-U_D}]\right\}. \quad (22b)$$

Thus, upon equating (22a) and (22b), one finds

$$\alpha_0 e^{U_{S0}-2U_F} - \alpha_L e^{U_{SL}-2U_F-U_D} = \frac{L_D}{x'_0}e^{-U_F/2}(U_{SL} - U_{S0}) + \sqrt{(U_{SL}-1)} - \sqrt{(U_{S0}-1)}. \quad (23)$$

Eliminating the α-related terms in eqn (21b) using eqn (23), and substituting the resulting expression into eqn (15), one finally obtains

$$I_D = \frac{Z\bar{\mu}_n C_0}{L}\left\{\left(V'_G + \frac{kT}{q}\right)(V_{SL} - V_{S0}) - \frac{1}{2}(V_{SL}^2 - V_{S0}^2) + V_B^2\left[\sqrt{(U_{SL}-1)} - \sqrt{(U_{S0}-1)} - \frac{2}{3}(U_{SL}-1)^{3/2} + \frac{2}{3}(U_{S0}-1)^{3/2}\right]\right\} \quad (24)$$

where

$$V_B^2 \equiv \left(\frac{kT}{q}\right)^2 \frac{x'_0}{L_D}\sqrt{\left(\frac{N_A}{n_i}\right)}. \quad (25)$$

Although established by a decidedly different approach, eqn (24) is precisely equivalent to eqn (11) of Ref. [5], the generalized charge-sheet result.

3. SAMPLE COMPUTATIONS

Sample computations were performed to numerically confirm the equivalence of the double and single integral theories, to investigate the accuracy of the charge-sheet expression, and to generally exhibit the utility of the eqn (15) result. Calculations were performed on a VAX 11/780 and all figures were computer generated. The integrals in eqn (15) were evaluated using the integration routine contained in the standard IMSL package.

Computed $I_D - V_D$ characteristics are displayed in Figs. 2(a) and 3(a). The device parameters assumed in constructing Fig. 2(a) were chosen to match a device described by Pao and Sah. Parameters typical of a modern but still long-channel MOSFET were assumed in constructing Fig. 3(a). Both figures contain two sets of curves, one computed from eqn (15) and the other based on the charge-sheet theory of eqn (24). The source and drain surface potentials in all cases were interpolated from the eqn (16) relationships.

As must be the case, the single integral results presented in Fig. 2(a) are identical to the double-integral curves shown in Fig. 2 of Pao and Sah. The charge-sheet relationship, moreover, is seen to be quite accurate in the triode and saturation regions of operation. A more precise appraisal of the approximate formula can be obtained from the fractional difference plots presented in Figs. 2(b) and 3(b); the largest computed error is only

†An accurate match to F_{max} is clearly desirable in evaluating the integrals in eqn (15). Also note that eqn (20) corresponds very closely to the first two terms in the expansion of eqn (18) when $\exp(U - U_F - \xi) \ll (U-1)\exp(U_F)$. This is required if the formalism is to yield the proper weak inversion dependence.

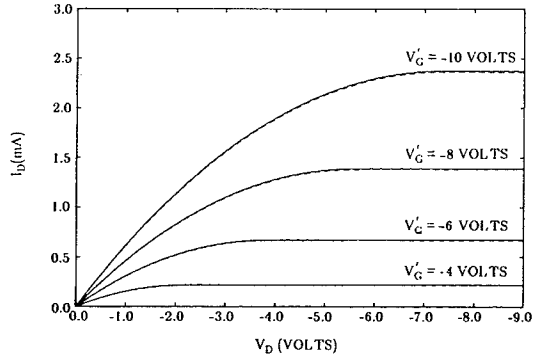

(a)

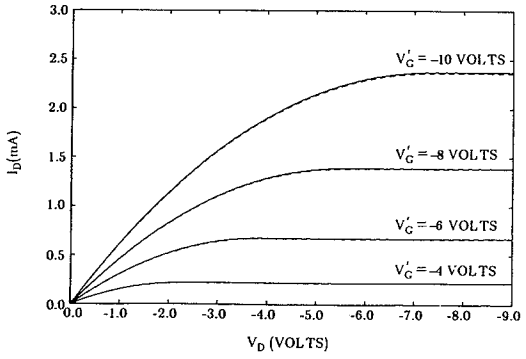

(b)

Fig. 2. (a) Theoretical $I_D - V_D$ characteristics of a p-channel MOS transistor described by Pao and Sah in Ref. [1]. $x_0 = 2000$ Å, $N_D = 4.6 \times 10^{14}/\text{cm}^3$, $\bar{\mu}_p = 256\ \text{cm}^2/\text{V-sec}$, $L = 70\ \mu\text{m}$, gate area $= 8.4 \times 10^{-4}\ \text{cm}^2$ and $T = 23°\text{C}$. The solid-line curves were computed using the single-integral expression, eqn (15), while the dashed-line curves were computed using the charge-sheet expression, eqn (24). In both cases, the source and drain surface potentials were calculated iteratively employing eqn (16). (b) Comparison between the single-integral and the charge-sheet computations of part (a). The percentage error is defined as $100\% \times [I_D(\text{integral}) - I_D(\text{charge-sheet})]/I_D(\text{integral})$.

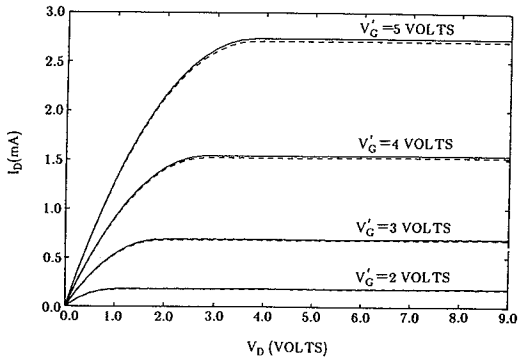

(a)

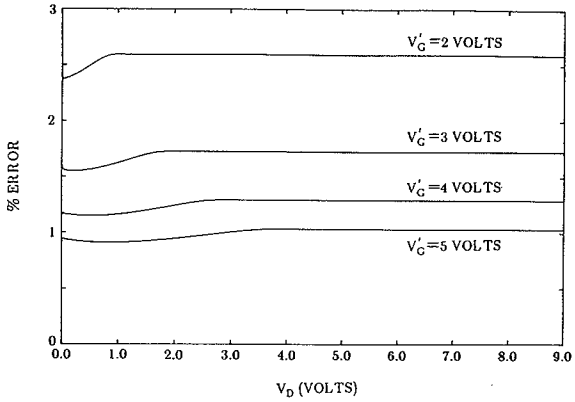

(b)

Fig. 3. (a) Theoretical $I_D - V_D$ characteristics of an n-channel MOS transistor with $x_0 = 500$ Å, $N_A = 1 \times 10^{15}/\text{cm}^3$, $\bar{\mu}_n = 550\ \text{cm}^2/\text{V-sec}$, $L = 7\ \mu\text{m}$, $Z = 70\ \mu\text{m}$, and $T = 23°\text{C}$. The solid-line curves were derived from the single-integral result while the dashed-line curves were computed from the charge-sheet expression. (b) Comparison between the single-integral and charge-sheet computations of part (a). The percentage error is as defined in Fig. 2.

2.7%. An interesting aspect of the Figs. 2 and 3 computation is the self-saturating nature of the charge-sheet theory. This feature in an approximate formulation follows from the proper computation of the surface potentials at the source and drain ends of the channel.

Computations of the subthreshold transfer characteristics, ln I_D vs V_G, are shown in Fig. 4. The experimental data also shown in Fig. 4 was taken from Fig. 33, p. 470 of Sze[2]. In effecting the comparison the theoretical characteristics were translated along the voltage axis to account for the nonzero flat-band voltages of the experimental devices. Needless to say, the charge-sheet formulation closely approximates the exact result which in turn is in excellent agreement with experiment. Somewhat larger charge-sheet errors are observed with decreasing substrate doping for gate biases at or slightly above the threshold point.

It should be mentioned that computations were also carried out using the eqn (19) bulk-charge relationship. When eqns (16) are used to compute the source and drain surface potentials, the bulk-charge theory is self-saturating. However, the fractional error was some two to four times greater than that exhibited by the charge-sheet theory. Moreover, the bulk-charge formulation is particularly inaccurate at and below the threshold voltage and as should be expected, yields highly inaccurate subthreshold transfer characteristics.

4. SUMMARY AND CONCLUDING COMMENTS

We have exhibited that the double-integral expression for the static characteristics of a long-channel MOSFET, a result which includes the diffusion component of the channel current and is continuously valid from weak inversion through saturation, can be reduced to a completely equivalent single-integral expression. Calculations based on the simplified integral expression are readily implemented, requiring little more computation time than approximate closed-form theories. Two approximate closed-form expressions, the bulk-charge and charge-sheet results, were shown to follow directly from the single integral relationship.

Computations presented herein simultaneously exhibit

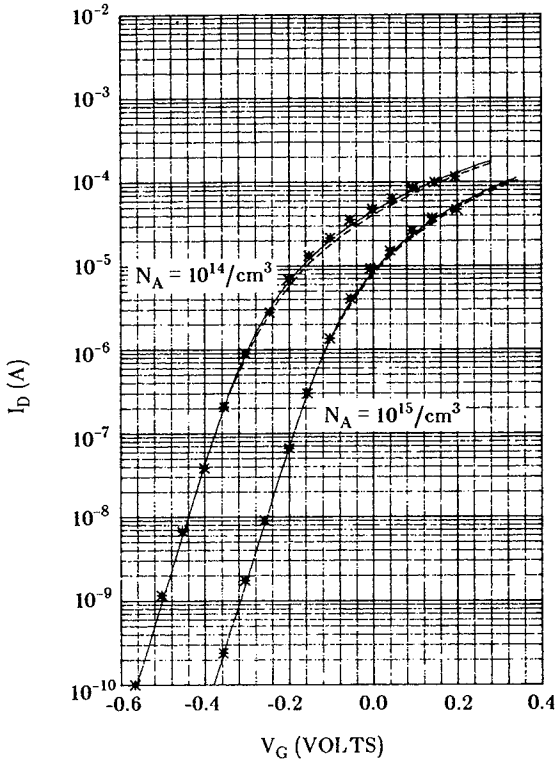

Fig. 4. The subthreshold transfer characteristics of *n*-channel MOSFET's having the same parameters as the Fig. 3 device except $N_A = 10^{14}/cm^3$ or $N_A = 10^{15}/cm^3$ and $x_0 = 130$ Å. The experimental data (*) was extracted from Fig. 33, p. 470 of Sze[2]. The solid and dashed-line curves were computed respectively from the single-integral and charge sheet expressions with $V_D = 1$ V. $V_{FB} = -0.92$ V for the $N_A = 10^{14}/cm^3$ device while $V_{FB} = -0.86$ V for the $N_A = 10^{15}/cm^3$ device.

the general utility of the single-integral result and independently confirm the high accuracy of the charge-sheet expression over the entire range of biases from weak inversion through saturation. These computational results, combined with the straightforward derivation of the charge-sheet expression, may provide greater acceptance and more wide-spread utilization of this excellent closed-form approximation.

Finally, as has been emphasized throughout, the theory considered herein is only valid for long-channel devices. Nevertheless, even with the advent of short-channel devices and short-channel effects, there remains a continuing utilization of long-channel and pseudo-long-channel models. Moreover, the observations cited herein may be of use in establishing improved models for short-channel devices.

Acknowledgement—This research was supported in part by the Air Force Office of Scientific Research under grant AFOSR-81-0214.

REFERENCES

1. H. C. Pao and C. T. Sah, *Solid-State Electron.* **9**, 927 (1966).
2. S. M. Sze, *Physics of Semiconductor Devices*, 2nd Edn. Wiley, New York (1981).
3. J. R. Brews, Physics of the MOS Transistor. In *Applied Solid State Science, Supplement* 2A. Academic Press, New York (1981).
4. T. Masuhara, J. Etoh and M. Nagata, *IEEE Trans. on Electron Dev.* **ED-21**, 363 (1974).
5. J. R. Brews, *Solid-St. Electronics.* **21**, 345 (1978).
6. C. T. Sah and H. C. Pao, *IEEE Trans. on Electron Dev.* **ED-13**, 393 (1966).